Journal of Anatomy

J. Anat. (2009) **214**, pp848–858 doi: 10.1111/j.1469-7580.2009.01077.x

A comparative study of the ocular skeleton of fossil and modern chondrichthyans

Brettney L. Pilgrim[1] and Tamara A. Franz-Odendaal[2]

[1]*Biology Department, Memorial University of Newfoundland, St. John's, Newfoundland, Canada*
[2]*Biology Department, Mount Saint Vincent University, Halifax, Nova Scotia, Canada*

Abstract

Many vertebrates have an ocular skeleton composed of cartilage and/or bone situated within the sclera of the eye. In this study we investigated whether modern and fossil sharks have an ocular skeleton, and whether it is conserved in morphology. We describe the scleral skeletal elements of three species of modern sharks and compare them to those found in fossil sharks from the Cleveland Shale (360 Mya). We also compare the elements to contemporaneous arthrodires from the same deposit. Surprisingly, the morphology of the skeletal support of the eye was found to differ significantly between modern and fossil sharks. All three modern shark species examined (spiny dogfish shark *Squalus acanthias*, porbeagle shark *Lamna nasus* and blue shark *Prionace glauca)* have a continuous skeletal element that encapsulates much of the eyeball; however, the tissue composition is different in each species. Histological and morphological examination revealed scleral cartilage with distinct tesserae in parts of the sclera of the porbeagle and blue shark, and more diffuse calcification in the dogfish. Strengthening of the scleral cartilage by means of tesserae has not been reported previously in the shark eye. In striking contrast, the ocular skeleton of fossil sharks comprises a series of individual elements that are arranged in a ring, similar to the arrangement in modern and fossil reptiles. Fossil arthrodires also have a multi-unit sclerotic ring but these are composed of fewer elements than in fossil sharks. The morphology of these elements has implications for the behaviour and visual capabilities of sharks that lived during the Devonian Period. This is the first time that such a dramatic variation in the morphology of scleral skeletal elements has been observed in a single lineage (Chondrichthyes), making this lineage important for broadening our understanding of the evolution of these elements within jawed vertebrates.
Key words arthrodires; bone; Chondrichthyes; cartilage; evolutionary developmental biology; scleral ossicles; sclera; tesserae.

Introduction

Sharks are considered to be one of evolution's 'success stories' as they have been swimming the oceans for more than 400 million years. Through this time they have survived mass extinctions that have wiped out other marine and terrestrial biota. As a result, we are left with 900–1100 living species of sharks (Compagno, 1990) – a highly diverse group in body size, habitat and feeding habits. In general, sharks are relatively large predators and as such help to shape the ecosystem due to the selective pressure they bring to bear (Compagno, 1990). Sharks are usually found at the top of their food web, and qualities such as well-developed eyes and well-developed non-visual senses (such as olfaction, electroreception and their acousticolateralis system) enable them to be supreme hunters (Compagno, 1990). Although the shark skeleton has been studied to some degree, the ocular skeleton has not been discussed.

In vertebrates the ocular skeleton (if present) consists of scleral cartilage and/or scleral ossicles; the presence and morphology of these elements vary amongst vertebrates (Franz-Odendaal & Hall 2006). Scleral skeletal elements belonging to reptiles [including birds (Modesto & Anderson, 2004)] have been investigated in the most detail, often using the chicken (*Gallus gallus*) as representative. Reptiles usually have both bone and cartilage within the sclera (Franz-Odendaal & Hall, 2006). In chickens, the sclerotic ring consists of 13–14 ossicles or flat bony plates that overlap one another to form the sclerotic ring (Walls, 1942). The sclerotic ring slightly overlaps a cup of scleral cartilage, which encapsulates most of the eyeball. The morphology of the sclerotic ring is influenced by the shape of the eyeball. Birds with tubular eyes, such as owls, have elongated, deep and concave ossicles, which contrast greatly with the flat, rhomboid-shaped ossicles of chickens (Curtis & Miller, 1938; Walls, 1942; Franz-Odendaal & Hall,

Correspondence
Tamara Franz-Odendaal, Biology Department, Mount Saint Vincent University, Halifax, Nova Scotia, B3 M 2J6, Canada.
E: Tamara.Franz-Odendaal@msvu.ca

Accepted for publication *6 March 2009*

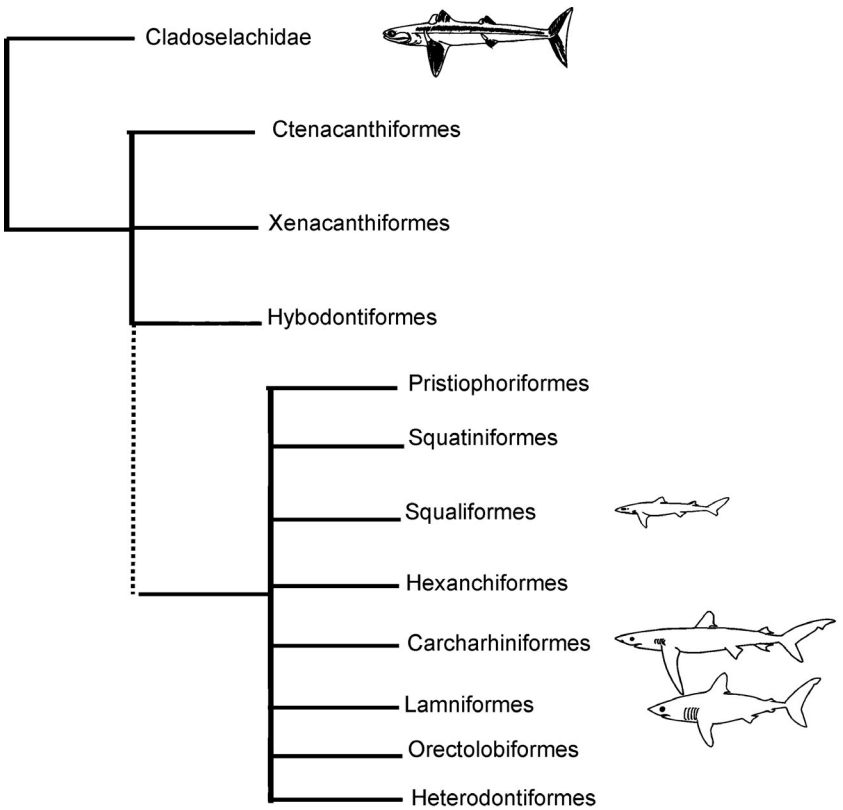

Fig. 1 Phylogeny showing the interrelationships of the sharks investigated in this study. Schematics show morphological similarities and differences between the species and relative maximum sizes (from Compagno, 1990). Spiny dogfish shark (Squaliformes: *Squalus acanthias*), blue shark (Carcharhiniformes: *Prionace glauca*) and porbeagle shark (Lamniformes: *Lamna nasus*). Fossil sharks are from Cladoselachidae and Ctenacanthiformes. Phylogeny is adapted from Nelson (2006) and Compagno et al. (2005).

2006). The number of individual ossicles that make up the sclerotic ring also varies amongst Reptilia, and within individual reptile species. Scleral skeletal elements serve to support and maintain the overall shape and rigidity of the eye. These elements protect the delicate internal tissues of the eye, including the lens, pigmented retina, and neural retina. Scleral ossicles in reptiles are, however, thought to play a role in accommodation, a process whereby the lens and cornea change shape to focus light onto the retina. The ossicles are thought to prevent distortion of the eyeball and thus maintain visual acuity (Lemmrich, 1931; Walls, 1942; King & McLelland, 1984).

Aquatic and amphibious organisms are faced with different visual challenges than purely terrestrial animals largely due to the fact that the refractive index of water is the same as that of the cornea. In diving birds, for example, the scleral ossicles are robust compared to non-diving birds, which typically have thin delicate sclerotic rings (Walls, 1942; Suburo & Scolaro, 1990). Entirely aquatic organisms (such as teleosts) accommodate differently in that the lens moves forwards and backwards and there is no distortion of the overall shape of the eye (Walls 1942), yet many teleosts have scleral ossicles (Nakamura & Yamaguchi, 1991). These ossicles, however, may not be developmentally homologous to those of reptiles (Franz-Odendaal & Hall, 2006).

To obtain insight into the ocular skeleton of sharks, we performed a morphological and histological assessment of the eye of three species of modern sharks (the spiny dogfish shark *Squalus acanthias*, the porbeagle shark *Lamna nasus* and the blue shark *Prionace glauca*). These three species vary in size, habitat, feeding habits, and in their interrelationships with other living and fossil sharks (Fig. 1). We then compare these skeletal elements to those of fossil sharks and other contemporaneous predators, namely the arthrodires, both of which are sister-groups to the rest of Gnathostomata (Fig. 6). We seek to understand whether the morphology of the ocular skeleton is conserved within Chondrichthyes and how they compare to those of the arthrodires. The ocular skeleton of modern sharks has not been investigated in detail to-date, although Walls (1942) reports that the sclera is thin in chimaeras and some deep-sea sharks and very thick in large sharks. This study sheds light on a skeletal element that is often overlooked within the vertebrate skeleton, yet one which can provide insight into the eye morphology and behaviour of fossil animals.

Materials and methods

Three species of modern shark were examined: *S. acanthias* (spiny dogfish shark), *P. glauca* (blue shark) and *L. nasus* (porbeagle shark). Frozen spiny dogfish shark specimens (FL 68 cm, caught at 44°14.10′N, 63°20.50′W) were obtained from Sambro Fisheries, Sambro, Nova Scotia. Frozen blue shark (two male sharks, FL 263 cm and 235 cm, caught off the shore of Liverpool, Nova Scotia) and porbeagle shark heads (two male sharks, one FL 158 cm

caught at 44°14.46′N, 61°21.43′W, the other, FL 179 cm at 44°12.95′N, 57°23.25′W) were obtained from the Bedford Institute of Oceanography, Bedford, Nova Scotia. Specimens were thawed and the eyeballs removed. Soft tissue within the eye was removed (e.g. lens, vitreous humour, etc.) and thick dense connective tissue fibres surrounding the scleral cup were dissected away to allow the stains to penetrate the scleral cup. The scleral cups were fixed in 10% neutral buffered formalin overnight and then transferred via a graded alcohol series to 70% ethanol for storage.

Fossil shark and arthrodire specimens from the Cleveland Shale (Devonian) were examined at the Cleveland Museum of Natural History in Cleveland, Ohio. Specimens are as follows: *Ctenacanthus* sp.: CMNH 5956; *Cladoselache* sp.: CMNH 5043, CMNH 5371, CMNH 5407, CMNH 5611, CMNH 5639, CMNH 5642, CMNH 5672, CMNH 5912, CMNH 6282, CMNH 7205, CMNH 8220, CMNH 8221, CMNH 8228, CMNH 8324, CMNH 8325, CMNH 8326, CMNH 9201, CMNH 9288; *Gymnotrachleus hydei*: CMNH 8051, CMNH 8052, CMNH 8053, CMNH 8055, CMNH 8799; *Paramylostoma arcualis*: CMNH 6054 (Holotype); Selenosteidae: one specimen (not catalogued); *Hoplonchus* sp.: CMNH 8108; *Titanichthys* sp.: CMNH 7075; *Heintzichthys* sp.: CMNH 8946, CMNH 8947, CMNH 8948, CMNH 8949, CMNH 8950, CMNH 475, CMNH I71a; *Heintzichthys gouldii*: CMNH 5291, CMNH 8056, CMNH 8057, CMNH 9311, CMNH 9405; *Dunkleosteus* sp.: CMNH 5012, CMNH 5108, CMNH 6220, CMNH 7217, CMNH 7568, CMNH 8800. In total, data were collected from 19 shark specimens [*Ctenacanthus* sp. (1), *Cladoselache fyleri* (18)] and 27 arthrodires [*Gymnotrachleus hydei* (5), *Paramylostoma arcualis* (1), Selenosteidae (1), *Hoplonchus* sp. (1), *Titanichthys* sp. (1), *Heintzichthys* sp. (7), *Heintzichthys gouldii* (5), *Dunkleosteus* sp. (6)]. Scleral skeletal elements were found as loose, fragmented plates, and/or embedded in shale.

Whole-mount and histological staining

A single scleral cup from each modern species was whole-mount stained for mineralization and/or cartilage using a slight modification of the staining protocol in Klymkowsky & Hanken (1991) and Franz-Odendaal et al. (2007). After staining, pieces of each scleral cup were dissected and viewed under a dissecting microscope (Nikon SMZ1500 Microscope) and photographs were taken using a Nikon DXM1200C Digital Camera.

In addition, two pieces of tissue (approximately 2–5 cm^2) from a single scleral cup of each species was decalcified in 18% EDTA (pH 7.2) for 2–4 weeks depending on the thickness of the scleral cup (*P. glauca* was decalcified for 4 weeks, *S. acanthias* for 2 weeks and *L. nasus* for 3 weeks). Following decalcification, the specimens were embedded in Paraplast Plus Wax (Fisher Scientific, #8889-502004) and sectioned at 10 μm. Slides were dewaxed and stained with either Masson's Trichrome Stain (consisting of haematoxylin, xylidene ponceau, phosphomolybdic acid and light green) (Flint & Lyons, 1975; Presnell & Schriebman, 1997; Witten & Hall, 2002; Franz-Odendaal et al. 2007) or Mallory's Trichrome Stain (consisting of saturated mercuric chloride, acid fuschin, phosphomolybdic acid and Mallory's stain) (Pantin, 1960; Franz-Odendaal et al. 2007). Sections were coverslipped with DPX Mountant (Fluka: 44581) and viewed with a Nikon Eclipse 50i Microscope. Photographs were taken using a Nikon DXM1200C Digital Camera.

Measurements and calculations

For modern sharks, the following measurements of the skeletal element were taken to calculate the approximate eye size and amount of scleral skeletal support: width, length and depth of the scleral cup, and width and length of the aperture (Fig. 2). Similar measurements were taken of the sclerotic ring of fossil sharks and arthrodires except that depth could not be measured; there was no evidence for the presence of a scleral cup in the fossil specimens we examined. An additional measure of a single scleral ossicle or plate was taken as shown in Fig. 2. All measurements were taken as maxima using electronic digital callipers (VWR Model 12777-830), and were recorded to the nearest 100th of a millimetre; results were rounded to the nearest 10th of a millimetre. A few fossil specimens were very fragmented, hence calculations using these measures underestimate the amount of scleral support.

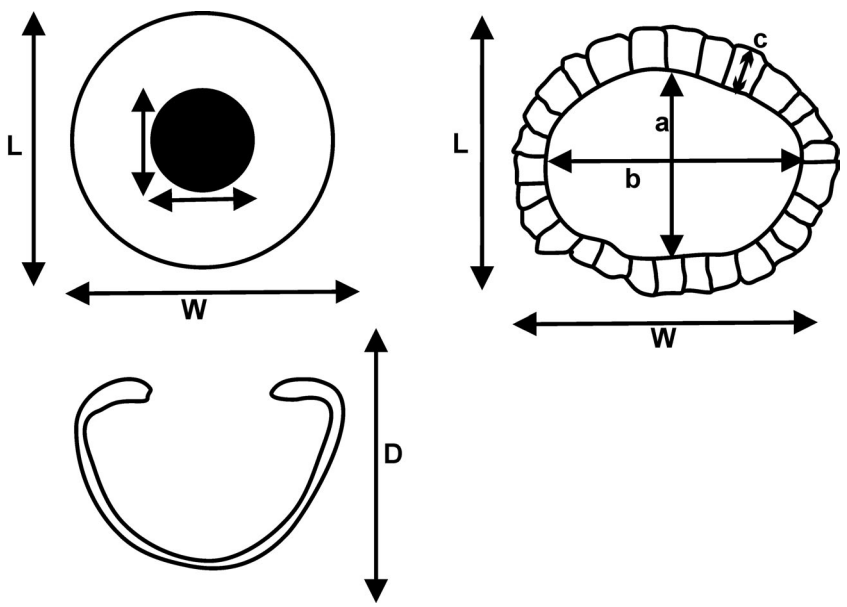

Fig. 2 Schematic of the surface view (top left) and lateral view (bottom left) of a modern shark scleral skeletal cup, and the surface view of a fossil scleral skeletal ring (top right). L, length of the scleral cup; W, width of the scleral cup; D, depth of the scleral cup; a, length of the aperture; b, width of the aperture; c, width of scleral skeletal plate/ring.

Table 1 Equations used to calculate the approximate surface area of the eye

Eq. 1	Surface area of a sphere	$= 4\pi r^2$ where $r^2 = (L{\cdot}W + L{\cdot}D + W{\cdot}D)/12$
Eq. 2	Surface area of the eye	$= \pi(L{\cdot}W + L{\cdot}D + W{\cdot}D)/3$
Eq. 3	Area of aperture	$= \pi{\cdot}(a/2){\cdot}(b/2)$
Eq. 4	Area with scleral skeletal support	= Surface area of eye – area of aperture

r, radius of a circle; L, length of scleral cup or ring; W, width of scleral cup or ring; D, depth of scleral cup or ring; a, aperture length; b, aperture width.

To quantify differences in scleral skeletal support between fossil and modern sharks, formulae were applied to measure the surface area of the eye and the percentage of the eye that had skeletal support (Table 1). Calculating the surface area of the eye was challenging as the shape of the eye is ellipsoid and there is no simple function to express the surface area of an ellipsoid. Hence, the area was approximated as a sphere using a similar method to Dall (1979), and the equations in Table 1. To calculate the percent of the eye with scleral skeletal support, the area of the aperture (Eq. 3) was subtracted from the total surface area of the sphere (Eq. 4) resulting in the area covered by scleral skeletal elements (Table 1). These values were then converted to percentages. Statistical analyses were performed using MINITAB (Version 15). For fossil specimens we could not measure depth of the eye due to compression during fossilization. We therefore approximated depth of the eyes using the average ratio (1.5) between the maximum length (L) and depth (D) of the scleral cups of the three modern shark species. This seemed reasonable as the standard deviation in the depth ratio of the three modern species is 0.06 despite significantly different body sizes (Table 2). In addition, it has been shown that eye size scales with body size in sharks (Lisney & Collins, 2007) and the fossil shark specimens we analysed are within the size range of the modern specimens (Long 1995; Janvier 1996). The assessment of the area of skeletal support for fossils is, however, an estimate, but it is nevertheless meaningful to graphically represent the dramatic differences in morphology with that of the modern species. For arthrodires, we used the same ratio (1.5) as their scleral ring sizes are larger than our modern shark eyes, indicating that arthrodires had larger eyes. As a proof of concept, if we use a depth value for arthrodires that is double that of the blue shark, the area of the eye increases and the percentage of skeletal support decreases. This has the effect of increasing the differences shown in Fig. 5. Therefore the differences shown are minimums.

Results

Modern chondrichthyes: gross morphology and histological analyses

The single scleral skeletal element found in the modern sharks is similar in each of the three modern species (spiny dogfish shark, porbeagle shark, blue shark) examined. It is in the form of a continuous cartilage cup that encapsulates the majority of the eye and is strengthened by mineralization in parts (e.g. in the portion of the sclera closest to the cornea, here referred to as the scleral-corneal limbus). This morphology is in contrast to what was observed in fossil specimens (discussed below).

Spiny dogfish shark: The spiny dogfish shark has the smallest scleral cup of all the modern species examined (Table 2). The cup is thin and flexible and composed entirely of hyaline cartilage (Fig. 3A–D). Histological analyses show that the hyaline cartilage is covered by a thick dense connective tissue. Chondrocytes are more densely packed and have flattened nuclei along the sides of the cartilage element below the perichondrium compared to interior regions, which have more cuboidal, loosely arranged cells (Fig. 3A). At the scleral-corneal limbus, however, the scleral cartilage cup is mineralized on the internal and external surfaces (Fig. 3D), and the perichondrium is thin (Fig. 3B). Corresponding areas of mineralization were observed in the whole-mount, undecalcified, specimen (not shown but see schematic Fig. 3D).

Blue shark and porbeagle shark: The blue shark and porbeagle shark have a larger scleral cartilage cup than the dogfish, as expected considering their larger body size (Table 2). Although the porbeagle has a smaller scleral cup and hence smaller eye than the blue shark, it has the largest aperture (Table 2). During gross dissection, we noticed that the scleral cup of the blue shark and porbeagle shark are thicker and more rigid than the element belonging to the spiny dogfish shark, yet all three are composed of hyaline cartilage (Fig. 3). With Alizarin red staining of undecalcified specimens we detected mineralized cartilage in two locations in the scleral cup of the blue and porbeagle shark (Fig. 3G,H,L,M). Similar to the spiny dogfish, the scleral-corneal limbus is reinforced with mineralization; however, the entire outer surface of the cartilage cup (furthest from retina) is also mineralized (compare

Table 2 Average measurements (in mm) of the scleral cup of the three modern shark species (spiny dogfish, *Squalus acanthias*; blue shark, *Prionace glauca*; porbeagle, *Lamna nasus*) (n = 2 for each species). D, L, W, a and b are shown in Fig. 2. Fork lengths as an indicator of body length are given in cm for each of the two specimens

	Spiny dogfish shark	Blue shark	Porbeagle shark
Depth (D)	18.2 ± 0.4	43.8 ± 4.2	34.8 ± 1.4
Length (L) × Width (W)	$27.8 \pm 1.1 \times 23.1 \pm 0.4$	$64.4 \pm 0.4 \times 62.8 \pm 2.6$	$55.6 \pm 0.3 \times 52.0 \pm 0.3$
Aperture (a × b)	$20.1 \pm 0.6 \times 13.6 \pm 1.2$	$30.2 \pm 3.6 \times 26.0 \pm 1.8$	$34.3 \pm 0.7 \times 30.0 \pm 1.0$
Body length	68–74	175–179	158–179

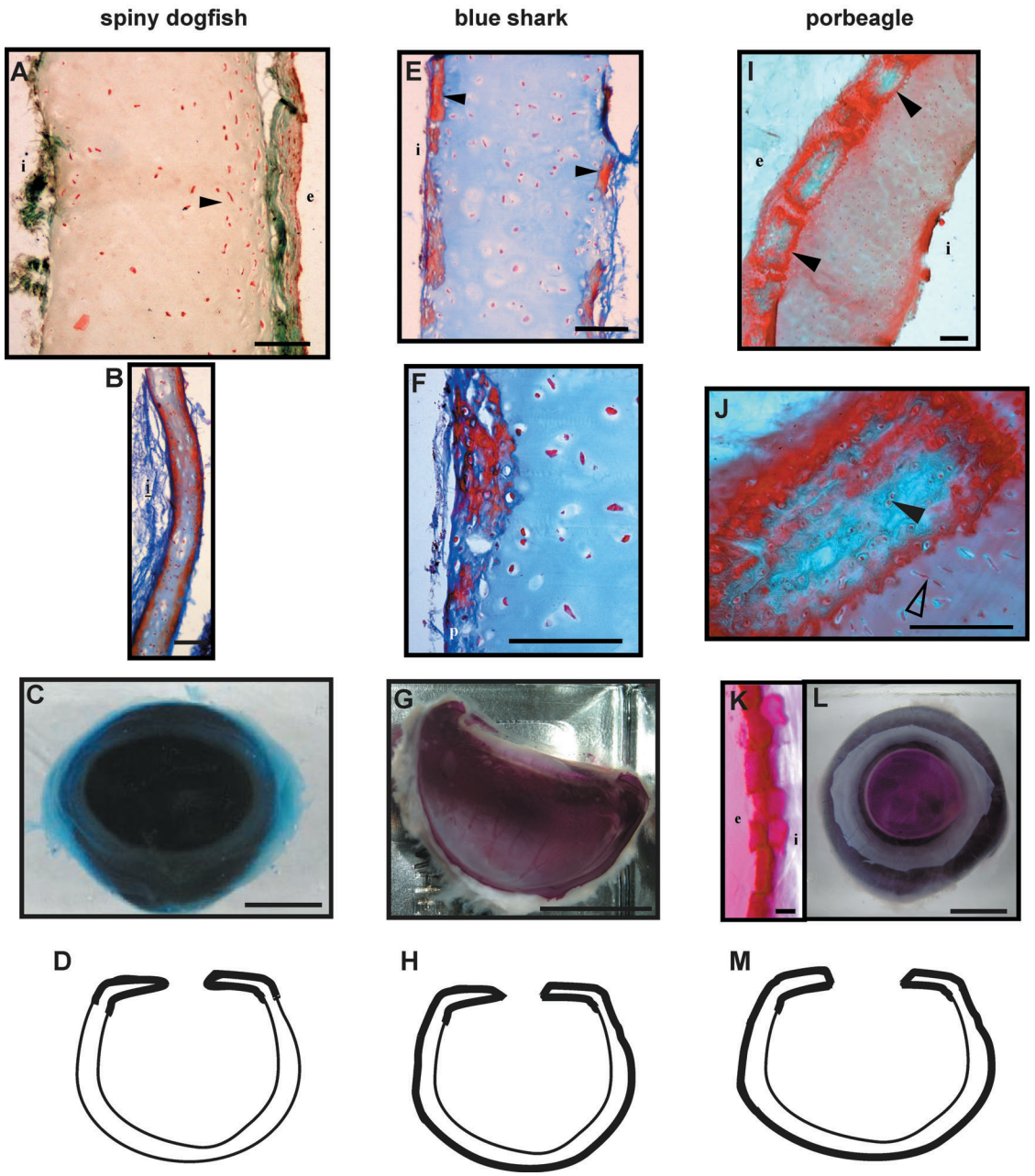

Fig. 3 Morphological and histological differences between the spiny dogfish shark (A–D), the blue shark (E–H) and the porbeagle shark (I–M) are shown. (A,B) Sections of the dogfish scleral skeletal element showing the thick hyaline cartilage core; arrowheads in A indicate denser aggregations of chondrocyte nuclei; Masson's Trichrome staining. (B) Scleral cartilage in the scleral-corneal limbus, Mallory's Trichrome staining. (C) *Squalus acanthias* scleral skeletal element whole-mount stained for cartilage with Alcian Blue. (D) Schematic of the dogfish eye; dark black lines show location of mineralization based on whole-mount stained specimens. (E) Sections of *Prionace glauca* scleral skeletal element stained with Mallory's Trichrome staining. Tesserae indicated by black arrowheads. (F) Enlarged view of tesserae. (G) *Prionace glauca* scleral cup cut in half; undecalcified and stained with Alizarin Red, showing mineralization. (H) Schematic of blue shark eye, dark black lines show where mineralization is located based on whole-mount stained specimens. (I,J) Longitudinal sections of *Lamna nasus*, the probeagle shark, stained with Masson's Trichrome staining. (I) Large blocks of tesserae (arrowheads) lining the exterior surface of the skeletal element. (J) Enlargement of (I). Tesserae have bright green to blue interiors and dark red boundaries indicative of mineralization. Cuboidal nuclei within tesserae are indicated by the solid arrowhead. Flat nuclei below and perpendicular to tesserae long axis are indicated by open arrowhead. (K) *Lamna nasus* scleral cup whole-mount stained with Alizarin Red cut to show the blocks of tesserae (mineralized) on the surface of the element. (L) *Lamna nasus* scleral stained with Alizarin Red. (M) Schematic of the porbeagle shark eye showing location of mineralization based on whole-mount stained specimens. Scale bars: (A,B,E,F,I,J) 100 μm, (C) 9 mm, (G,L) 18 mm, (K) 200 μm. i, interior of eye; e, exterior of eye.

Table 3 Comparison of the histology and whole-mount staining of the ocular skeleton in the three species of modern sharks. In all species, the ocular skeleton consists of a cartilage core element with a thin perichondrium; between these two tissues, tessarae may be present

	Cartilage core	Tesserae
Spiny dogfish shark (*Squalus acanthias*)	Cellular with some hypertrophic cells; lacunae are distinct	Some partial mineralization at edges of core (below perichondrium); no distinct tesserae
Blue shark (*Prionace glauca*)	Not very cellular; slightly more cellular closer to edges (perichondrium); lacunae are distinct	Tesserae are less distinct and rectangular; tesserae are not organized and consist of mineralized matrix with few cells; tesserae make up 1/8th of width of the scleral cartilage
Porbeagle shark (*Lamna nasus*)	Internal region is not very cellular; closer to the edges (perichondrium) it is slightly more cellular; lacunae are not distinct	Tesserae are very distinct large square blocks; tesserae are densely mineralized and organized; nuclei and lacunae are observed within tesserae; region between tesserae is cellular similar to regions below (internal to) the tesserae; tesserae make up 1/5th of width of the scleral cartilage

Table 4 Measurements (in mm) of the sclerotic ring of the fossil sharks and arthrodires analysed

		No. of plates/eye	Shape	Aperture size	Ring size	Width of ring
Sharks	*Ctenacanthus* sp.	Not det.	oval	36.5×23.2 ($n = 1$)	–	7.6 ± 4.4 ($n = 4$)
	Cladoselache sp.	24 ± 8 ($n = 12$)	oval	20.8 ± 7.3 ($n = 7$) $\times 12.3 \pm 6.3$ ($n = 9$)	49.1×45.4 ($n = 1$)	3.5 ± 1.5 ($n = 30$)
Arthrodires	*Gymnotrachleus hydei*	4 ($n = 1$)	circular	42×42 ($n = 1$)	–	13.6 ± 1.4 ($n = 7$)
	Paramylostoma arcualis	Not det.	oval	25.7×21.0 ($n = 1$)		14.7 ($n = 1$)
	Selenosteidae	Not det.	oval	$21.9 \pm 3.3 \times 10.7 \pm 1.4$ ($n = 2$)	38.4 ($n = 1$)*	12.1 ($n = 1$)
	Hoplonchus sp.	5–12	oval	39.1×29.2 ($n = 1$)	–	17.1** ($n = 1$)
	Titanichthys sp.	4 ($n = 1$)	circular	–	–	28.1 ± 2.2 ($n = 5$)
	Heintzichthys sp.	Not det.	oval	36.7 ± 9.1 ($n = 3$) $\times 29.1$ ($n = 1$)	153.0×77.7 ($n = 1$)	20.6 ± 8.2 ($n = 10$)
	Heintzichthys gouldii	4 ($n = 3$)	oval	$38.6 \pm 1.9 \times 29.0 \pm 3.0$ ($n = 5$)	$88.0 \pm 3.3 \times 79.7 \pm 5.4$ ($n = 2$)	28.0 ± 5.2 ($n = 15$)
	Dunkleosteus sp.	4 ($n = 4$)	circular	$20.0 \pm 3.6 \times 20.0 \pm 3.6$ ($n = 6$)	$69.0 \pm 5.5 \times 69.0 \pm 5.5$ ($n = 3$)	28.2 ± 3.0 ($n = 17$)

n, number of specimens or plates measured; Not det., dimensions that could not be measured due to severe fragmentation.
All measurements are maximums.
*Only one dimension could be measured in this specimen.
**This is a minimum measurement.

Fig. 3D,H,M schematics). The mineralization observed in whole-mount stained specimens is in the form of blocks, or tesserae (Fig. 3). In the blue shark, tesserae are observed both in whole-mount stained specimens (not shown) and in histological sections (Fig. 3E,F). The tesserae are flat and irregularly shaped with no distinct core (compare Fig. 3E and I). In the porbeagle, the cartilage core is mineralized and the tesserae are highly organized blocks (unlike in the blue shark) (Fig. 3I–J). Lies lines as described in Dean & Summers (2006) appear to be present within some tesserae (Fig. 3K). The area between adjacent tesserae is narrow and contains dense matrix. The density of cells (chondrocytes) is also greater within the tesserae than internally within the hyaline cartilage core. In addition, in the blue shark the hyaline cartilage core is uncalcified (data not shown), similar to that seen in the dogfish but unlike that in the porbeagle.

In summary, the tissue morphology of the scleral cartilage is similar in each of the three species in that it consists of a hyaline cartilage core with some denser, mineralized areas below a thin perichondrium (summarized in Table 3, Fig. 3). The amount and location of mineralization is variable in the three modern species, from sparse in the dogfish, to irregular in the blue shark, to highly organized in the porbeagle.

Fossil specimens

The data for fossil specimens is summarized in Table 4 and shown in Fig. 4. In only two genera of fossil sharks at the Cleveland Museum were scleral ossicles found – 18 *Cladoselache* sp. (see above for specimen numbers) and a single *Ctenacanthus* sp. specimen (CMNH 5956) were examined. The ocular skeleton of these two fossil sharks is in the form of a ring that is oval in shape, and does not encapsulate the entire eyeball (as a cup) as observed in modern sharks. In the *Ctenacanthus* specimen the number of plates could not be determined; however, in *Cladoselache* we observed 24 ± 8 small, rectangular plates per eye (Table 4, Fig. 4B).

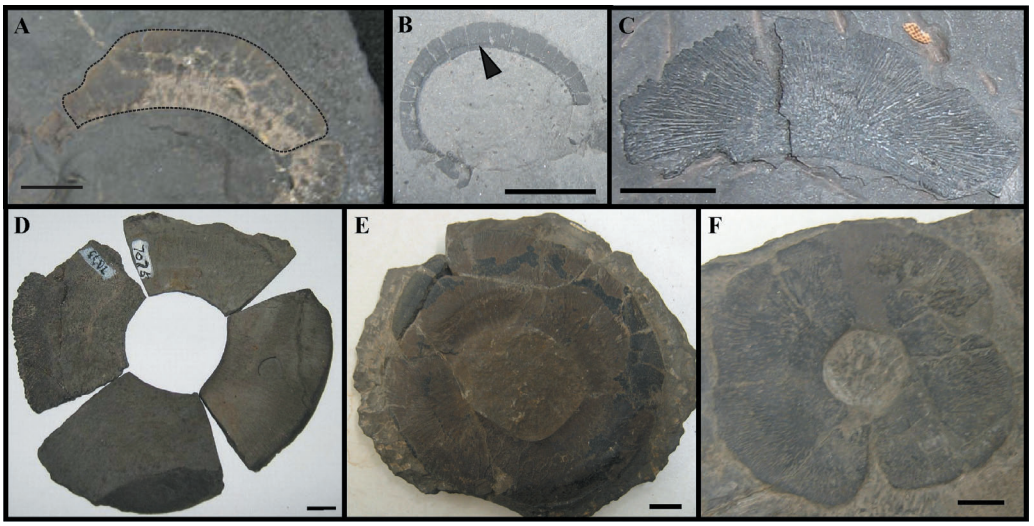

Fig. 4 Fossil specimens. (A) Scleral plate belonging to *Ctenacanthus* sp. CMNH 5956. Dotted line indicates the boundary of the scleral plate. (B) Partial scleral ring of *Cladoselache* sp. CMNH 8324 composed of many small rectangular plates (single plate indicated by arrowhead). (C) *Gymnotrachleus hydei* scleral plate, CMNH 8053, crescent-shaped with tapered ends. (D) Four *Titanichthys* sp. sclerotic plates arranged into a sclerotic ring. (E,F) *Heintzichthys gouldii* sclerotic ring CMNH 5291. All scale bars are 10 mm.

Among the arthrodire collection, we examined five *Gymnotrachleus hydei*, one *Paramylostoma arcualis*, one member of the family Selenosteidae, 12 *Heintzichthys,* one *Hoplonchus,* one *Titanichthys* and six *Dunkleosteus* specimens. Similar to fossil sharks, the ocular skeleton is in the form of a multi-component ring and does not completely encapsulate the eyeball as a single skeletal element, as it does in modern sharks. The shape of the sclerotic ring was circular or oval, and does not appear to correlate with aperture size or width of the sclerotic ring (Table 4). In four genera of arthrodires (17 specimens) four scleral ossicles per eye were consistently present. The exception was *Hoplonchus*, which had 5–12 ossicles per eye; however, this count is based on a single incomplete specimen. The largest sclerotic ring was observed in *Heintzichthys* sp., and the widest ring was found in *Titanichthys* sp. The aperture and ring size of this *Titanichthys* specimen could not be determined and may have exceeded that observed in *Heintzichthys* sp.

Estimate of eye size and quantity of scleral skeletal support

Overall, the morphology of the scleral skeletal elements in the three groups examined (modern sharks, fossil sharks and arthrodires) varied significantly. A complete skeletal cup is present in modern sharks, a narrow sclerotic ring is present in fossil sharks and a wide sclerotic ring is present in arthrodires (Fig. 6). Similarly, the percentage of scleral support also varied significantly [F (2,10) = 160.3, $P < 0.001$] (Fig. 5).

The eyes of the fossil sharks are significantly smaller than those of modern sharks and most of the arthrodires

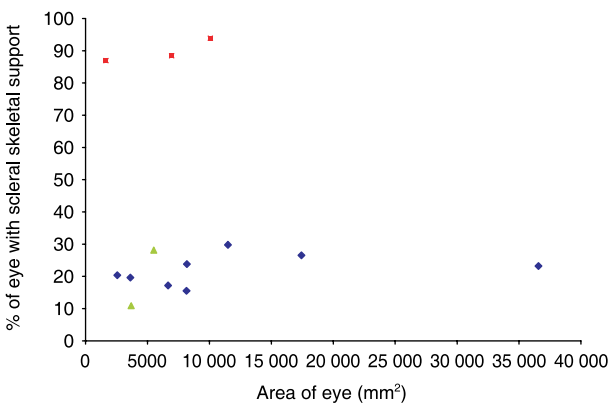

Fig. 5 Scatter plot showing the relationship between eye surface area and percentage of the eye with scleral skeletal support in modern sharks (red squares), fossil sharks (green triangles) and arthrodires (blue diamonds).

(namely *Heintzichthys* and *Titanichthys*) (Tables 4 & 5). The fossil sharks have the smallest eyes, whereas the arthrodire *Heintzichthys* sp. has the largest (Table 5). The percentage of scleral skeletal support is significantly greater in the modern sharks (87–94%) than all other specimens examined, which are below 30% supported (Fig. 5). Our estimated percentage of skeletal support for the arthrodires ranges from as little as 15% in *G. hydei* to almost 30% in those specimens with large eyes such as in *Dunkleosteus*. Fossil sharks have the lowest percentage of scleral skeletal support (11–28%). The estimated fossil shark eye surface areas are larger than that of the dogfish and below the value for the porbeagle, yet the percentage of scleral support in fossil sharks is significantly lower (11–28% compared to over 86%). In general, within each group,

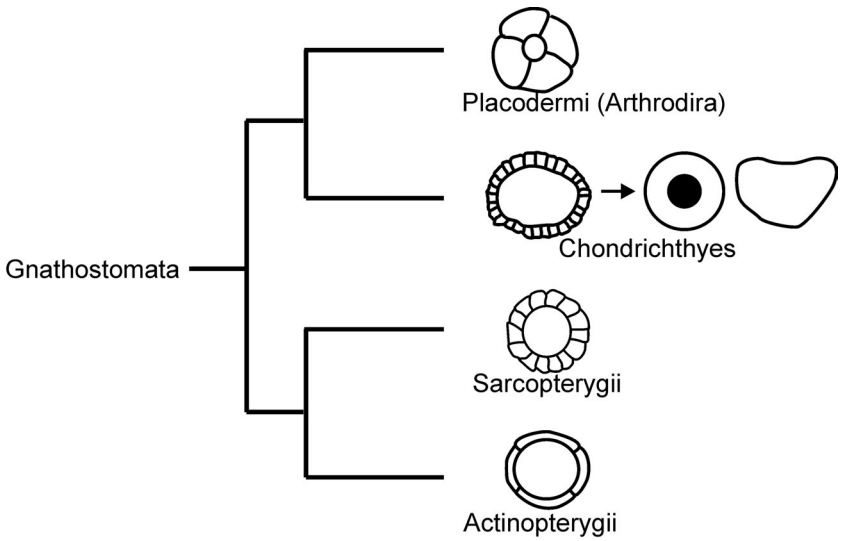

Fig. 6 Schematics of the scleral skeletal support belonging to Placodermi (including arthrodires), Chondrichthyes (fossil to modern sharks), basal Sarcopterygii (reptiles) and basal Actinopterygii. Adapted from Franz-Odendaal & Hall (2006).

Table 5 Percentage of scleral skeletal support and eye surface area calculated from measurements and equations reported in Tables 1, 2, and 4 and described in our methodology

	Genera	Area of eye (mm^2)	% of eye with skeletal support
Arthrodires	*Paramylostoma arcualis*	3 612	19.6
	Titanichthys sp.	8 178	23.8
	Heintzichthys gouldii	17 433	26.6
	Heintzichthys sp.	36 579	23.2
	Dunkleosteus sp.	11 495	29.8
	Gymnotrachleus hydei	8 150	15.5
	Selenosteidae	2 563	20.4
	Holplonchus sp.	6 663	17.2
Fossil sharks	*Ctenacanthus* sp.	3 680	10.9
	Cladoselache sp.	5 506	28.1
Modern sharks	*Squalus acanthias* (spiny dogfish)	1 643	86.9
	Prionace glauca (blue shark)	10 070	93.9
	Lamna nasus (porbeagle)	6 949	88.4

there is a positive correlation between the eye area and the amount of skeletal support (Fig. 5).

Discussion

A shared feature of extant elasmobranchs (sharks and rays) is that they have entirely cartilaginous skeletons, yet these are often heavily mineralized. Mineralization is in the form of prisms of crystalline calcium phosphate in discrete blocks, called tesserae, located on the surface of the cartilages (Kemp & Westrin 1979; Dingerkus et al. 1991; Summers et al. 1998). The tesserae typically form a continuous mosaic between a thin perichondrium and a hyaline cartilage core. Tesserae consist of two types of calcification – globular (inner) and prismatic (outer) (Dean & Summers, 2006). Cartilage with tesserae is called tessellated cartilage by some authors (Dean & Summers, 2006). The functional significance of tesserae is to stiffen the skeleton (Dingerkus et al. 1991; Dean et al. 2006; Dean & Summers, 2006). Although tesserae are reported in several regions of the chondrichthyan skeleton [e.g. vertebral column (Ridewood, 1921; Ørvig, 1951; Eames et al. 2007) and jaws (Dingerkus et al. 1991; Summers, 2000; Dean et al. 2006)], they have not been reported in the eye.

Here we show that tessellated cartilage is present in the ocular skeleton of some extant sharks. That is, the cartilage in the eye of sharks has stiffened in different ways, probably depending on the functional requirements (discussed below). In all three species examined, the ocular skeleton is strengthened at the scleral-corneal limbus to varying degrees. This region is often the thinnest area of the scleral cup and is also the area subject to the greatest water pressure during fast swimming as it is the most exposed to the external environment (unlike the rest of the eye, which is protected within the eye socket) (Walls, 1942; Franz-Odendaal & Hall, 2006).

We then asked whether the ocular skeleton relates to behaviour or affects visual acuity. The two more active predators in this study, the porbeagle shark and the blue shark, are pelagic, fast-swimming species of sharks that feed on active, mobile prey (Compagno et al. 2005). These two species have more scleral skeletal support (stiffened by tesserae) than does the spiny dogfish shark (Fig. 3), which is a benthic, slow-swimming species (Compagno et al. 2005). Porbeagle and blue sharks eat similar diets; however, porbeagle sharks predominately eat fast-swimming squid, shellfish and pelagic fishes (herring, mackerel, etc.) and inhabit continental shelves, whereas blue sharks eat many types of pelagic fish and seals, and inhabit a wide range of pelagic zones. The porbeagle is, however, warm-bodied, unlike the blue shark (and dogfish shark), and can generate greater power needed for high-speed swimming (Joyce et al. 2002). It also has more discrete, organized tesserae than

the blue shark. It therefore appears that the degree of stiffening required in the scleral cup may be correlated with activity level (i.e. high-speed swimming), the more active faster swimming sharks having a greater need for scleral support than do smaller, more benthic slower species.

The relationship between activity level and scleral skeletal support has been investigated in other aquatic vertebrates, namely teleosts (Franz-Odendaal, 2008). The majority (80%) of the teleost families examined were sluggish (low activity level) and had no scleral ossicles, whereas all families that were very active had scleral ossicles. Robust scleral skeletal support is also reported in other vertebrates that are described as being very active, such as fast-flying birds of prey (Walls, 1942), and swift-swimming fish (e.g. tuna and swordfish) (Nakamura & Yamaguchi, 1991). Ichthyosaurs, a group of extinct marine reptiles, have features that indicate they may have been swift swimmers (e.g. a streamlined body) (Massare & Callaway, 1990), and they also have well-developed scleral ossicles (Motani et al. 1999).

The trend for more active, faster swimming sharks to have increased scleral skeletal support (distribution and organization of tesserae) is, however, not found in the fossil sharks examined in this study. *Cladoselache* has been classified alongside modern sharks (such as the long-finned mako) as a macroceanic species (Compagno, 1990); it is estimated to be about 100 cm in body length (Long 1995). These fossil sharks are therefore portrayed as active, fast-swimming pelagic species. However, *Cladoselache* has very little scleral skeletal support, as evidenced by its tiny scleral plates compared to the active, pelagic modern species in this study (e.g. the porbeagle shark and blue shark) (Fig. 5). With regard to the strength of their ocular skeleton it is unknown at present whether the scleral elements in the fossil sharks are composed of mineralized cartilage or possibly bone. In addition, we could find no evidence for an additional skeletal element encapsulating the eyeball. This lack of correlation between the amount of scleral support and activity level is not surprising when one considers the strikingly different morphology of the ocular skeleton; this morphology may, however, correlate with enhanced visual capabilities.

In some vertebrates, namely reptiles, visual acuity is affected by scleral support – in reptiles, scleral ossicles play a role in accommodation (Lemmrich, 1931; Walls, 1942; King & McLelland, 1984). The similar morphology of the ocular skeleton in fossil sharks (to that in reptiles, a ring composed of flat, rectangular overlapping plates [Fig. 6]) could suggest that they, too, may have had the same mode of accommodation. It is also recognized that modern sharks have a well-developed visual system (Gruber et al. 1963; Hamasaki & Gruber, 1965; Gruber & Cohen, 1978; Hueter & Cohen, 1991; Hart et al. 2006). At least one modern shark has been shown to be emmetropic (i.e. the lens is focused on objects in the distance) at rest (lemon shark: Hueter et al. 2001) and can accommodate by moving its lens away from the cornea, towards the retina, similar to reptiles (Schaeffel, 1994; Glasser, 2003). In summary, modern sharks have a limited ability to accommodate by moving the lens despite significant (yet potentially flexible) scleral support. Fossil sharks, on the other hand, have a similar ocular skeletal morphology to that of modern reptiles (Franz-Odendaal & Hall, 2006) and may therefore also have been able to accommodate; perhaps more readily than modern sharks. This ability to accommodate the eye could have provided fossil sharks with the acute vision they needed to compete against their massive marine predators, such as *Dunkleosteus*. Over evolutionary time, this mode of accommodation was lost within shark lineages, perhaps as a trade-off to evolving a large eye, which offers other advantages for increased visual acuity.

Some of the arthrodires examined in this study were large, active marine predators. For example, *Dunkleosteus* is presumed to have been a swift swimmer in order to prey upon fast-swimming, active fossil sharks (Carr, 1995). Arthrodires seem to follow the trend that more active animals tend to have increased scleral skeletal support (38% support). The four-component sclerotic ring of arthrodires noted here as well as the fused scleral ring of small placoderms (Burrow et al. 2005) are significantly wider than the thin sclerotic ring of fossil sharks and therefore offer a larger amount of support to the delicate eye tissues. The functional significance of this morphology is not understood at present; the ability of arthrodires to adjust the curvature of the cornea or move the lens may have been limited due to this wider bony scleral element. Ultimately, this would have decreased their visual acuity compared to the contemporaneous fossil sharks, which were generally smaller in body size and fast swimmers (Carr 1995; Long 1995; Janvier 1996).

The data presented here provides significant insight into the evolution of the ocular skeleton (Fig. 6), a region that is often overlooked by both anatomists and paleontologists. In basal Actinopterygii, the ocular skeleton consisted of four elements; in Sarcoptergyii this region was composed of over 20 bones; and in Placodermi there are typically four bones per eye. Clearly this region of the skeleton is variable in morphology in several lineages. This study sheds light on the ocular skeleton within Chondrichthyes, which has undergone the most dramatic variation from a multi-component ring to a solid capsule. It has been suggested that the ocular skeleton of teleosts may not be homologous to those of sarcopterygians (Franz-Odendaal & Hall, 2006); similarly, the elements within the chondrichthyan lineage require further investigation to determine the homology between the different morphologies revealed here.

Concluding remarks

This study found that the scleral skeletal support found in *S. acanthias*, *L. nasus* and *P. glauca* is in the form of a

continuous hyaline cartilage cup that encapsulates most of the eye (86–94% of the eye). This cartilage element is partially surrounded by tesserae in *L. nasus* and *P. glauca*, but not in *S. acanthias*, with some form of calcification present at the scleral-corneal limbus in all three species. Tesserae have not been previously reported in the ocular skeleton of modern sharks. Tessellated cartilage provides stronger support for the sclera of the eye (compared to regular hyaline cartilage) in the larger, more active species.

The scleral skeletal support of fossil sharks was significantly different in morphology to that found in modern sharks. Fossil sharks have scleral skeletal support in the form of a sclerotic ring, which does not encapsulate the eyeball as does the scleral cup of modern sharks. This was surprising because a change in the morphology of the scleral skeletal support within one lineage has not been observed previously. The morphology of the sclerotic ring found in fossil sharks is very similar to that seen in reptiles. As it is thought that the sclerotic ring in reptiles plays a role in accommodation, the similar morphology of the fossil shark sclerotic ring suggests that fossil sharks may have accommodated in a similar manner to reptiles. The increase in scleral skeletal support found in modern sharks may have been an evolutionary trade-off for the eye to become very large in some species (e.g. the porbeagle shark and the blue shark). The data from this research are significant because they describe the variation between the morphologies of scleral skeletal elements in modern and fossil sharks compared to fossil arthrodires. It is important to document the variation in morphology of these elements in gnathostomes to broaden our understanding of the evolution of the ocular skeleton. This study, although not an exhaustive study of all shark species, provides some novel insights into the evolution of scleral ossicles, and the distribution of tessellated cartilage amongst chondrichthyans.

Acknowledgements

This research was supported by an NSERC Discovery Grant and a Journal of Experimental Biology Travel Fellowship to T.F.O. to study the fossil sharks. We would like to thank Michael Ryan and Gary Jackson for their assistance with the collection at the Cleveland Museum of Natural History (Ohio, USA). We wish to thank Steven Campana (Marine Fish Division, Bedford Institute of Oceanography, Nova Scotia, Canada) and Sambro Fisheries (Nova Scotia, Canada) for supplying the modern shark specimens. We are grateful to the reviewers for valuable comments on earlier versions.

References

Burrow CJ, Jones AS, Young GC (2005) X-ray microtomography of 410 million year old optic capsules from placoderm fishes. *Micron* **36**, 551–557.

Carr RK (1995) Placoderm diversity and evolution. *Bull Mus Natl Hist Nat, Section C* **17**, 85–125.

Compagno LJV (1990) Alternative life-history styles of cartilaginous fishes in time and space. *Environ Biol Fishes* **28**, 33–75.

Compagno LJV, Dando M, Fowler S (2005) *Sharks of the World*. p. 368. Princeton: Princeton Field Guides, Princeton University Press.

Curtis EL, Miller RC (1938) The sclerotic ring in North American birds. *Auk* **55**, 225–243.

Dall PC (1979) A sampling technique for littoral stone-dwelling organisms. *Oikos* **33**, 106–111.

Dean MN, Summers AP (2006) Mineralized cartilage in the skeleton of chondrichthyan fishes. *Zoology* **109**, 164–168.

Dean MN, Huber DR, Nance HA (2006) Functional morphology of jaw trabeculation in the lesser electric ray Narcine brasiliensis, with comments on the evolution of structural support in the Batoidea. *J Morphol* **267**, 1137–1146.

Dingerkus G, Seret B, Guilbert E (1991) Multiple prismatic calcium phosphate layers in the jaws of present-day sharks (Chondrichthyes; Selachii). *Experientia* **47**, 38–40.

Eames BF, Allen N, Young J, Kaplan A, Helms JA, Schneider RA (2007) Skeletogenesis in the swell shark *Cephaloscyllium ventriosum*. *J Anat* **210**, 542–554.

Flint MH, Lyons MF (1975) The effect of heating and denaturation on the staining of collagen by the Masson's trichrome procedure. *Histochem J* **7**, 547–555.

Franz-Odendaal TA (2008) The scleral ossicles of teleostei: evolutionary and developmental trends. *Anat Rec* **291**, 161–168.

Franz-Odendaal TA, Hall BK (2006) Skeletal elements within teleost eyes and a discussion of their homology. *J Morphol* **267**, 1326–1337.

Franz-Odendaal T, Ryan K, Hall B (2007) Developmental and morphological variation in the teleost craniofacial skeleton reveals an unusual mode of ossification. *J Exp Zool* **308B** (Mol Dev Evol), 709–721.

Glasser A (2003) How other species accommodate. In *Current aspects of Human Accommodation II* (eds Guthoff R, Ludwig K), pp. 13–38. Heidelberg: Kaden Verlag.

Gruber SH, Cohen JL (1978) Visual system of the elasmobranchs: state of the art. In *Sensory Biology of Sharks, Skates and Rays* (eds Hodgson ES, Mathewson RF), pp. 11–116. Washington, D.C.: US Government Printing Office.

Gruber SH, Hamasaki DI, Bridges CDB (1963) Cones in the retina of the lemon shark *(Negaprion brevirostris)*. *Vision Res* **3**, 397–399.

Hamasaki DI, Gruber SH (1965) The photoreceptors of the nurse shark *Ginglymostoma cirratum* and the sting ray, *Dasyatis sayi*. *Bull Mar Sci* **15**, 1051–1059.

Hart NS, Lisney TJ, Collin SP (2006) Visual communication in elasmobranchs. In *Communication in Fishes* (eds Ladich F, Collin SP, Moller P, Kapoor BG), pp. 337–392. Enfield, NH: Science Publishers Inc.

Hueter RE, Cohen JL (1991) Vision in elasmobranchs: a comparative and ecological perspective. *J Exp Zool Suppl* **5**, 1–182.

Hueter RE, Murphy CJ, Howland M, Sivak JG, Paul-Murphy JR, Howland HC (2001) Refractive state and accommodation in the eyes of free-swimming versus restrained juvenile lemon sharks (*Negaprion brevirostris*). *Vision Res* **41**, 1885–1889.

Janvier P (1996) *Early Vertebrates*. Oxford: Oxford University Press.

Joyce WN, Campana SE, Natanson LJ, Kohler NE, Pratt HL, Jensen CF (2002) Analysis of stomach contents of the porbeagle shark (Lamna nasus Bonnaterre) in the northwest Atlantic. *ICES J Mar Sci* **59**, 1263–1269.

Kemp NE, Westrin SK (1979) Ultrastructure of calcified cartilage in the endoskeletal tesserae of sharks. *J Morphol* **160**, 75–102.

King AS, McLelland J (1984) *Birds, Their Structure and Function* 2nd edn. London: Bailliere Tindal.

Klymkowsky MW, Hanken J (1991) Whole-mount staining of *Xenopus* and other vertebrates. *Methods Cell Biol* **36**, 419–441.

Lemmrich W (1931) Die Skleralring der Vögel *Jena Z Naturwiss* **65**, 513–586.

Lisney TJ, Collins SP (2007) Relative eye size in Elasmobranchs. *Brain Behav Evol* **69**, 266–279.

Long JA (1995) *The Rise of Fishes*. Baltimore: Johns Hopkins University Press.

Massare JA, Callaway JM (1990) The affinities and ecology of Triassic ichthyosaurs. *GSA Bull* **102**, 409–416.

Modesto SP, Anderson JS (2004) The phylogenetic definition of reptilia: systematic biology. *System Biol* **53**, 815–821.

Motani R, Rothschild BM, Wahl W (1999) Large eyeballs in diving ichthyosaurs. *Nature* **402**, 747.

Nakamura K, Yamaguchi H (1991) Distribution of scleral ossicles in teleost fishes. *Mem Fac Fisheries Kagoshima Univ* **40**, 1–20.

Nelson JS (2006) *Fishes of the World*. New York: John Wiley & Sons, Inc.

Ørvig T (1951) Histologic studies of Placoderms and fossil Elasmobranchs. I. The endoskeleton, with remarks on the hard tissues of lower vertebrates in general. *Ark Zool* **2**, 321–454.

Pantin CFA (1960) *Notes on Microscopical Technique for Zoologists*. Cambridge: Cambridge University Press.

Presnell JK, Schriebman MP (1997) *Humason's Animal Tissue Techniques*. Baltimore: Johns Hopkins University Press.

Ridewood WG (1921) On the calcification of the vertebral centra in sharks and rays. *Philos Trans R Soc Lond B* **210**, 311–407.

Schaeffel F (1994) Functional accommodation in birds. In *Perception and Motor Control in Birds* (eds Davies MNO, Green PR), pp. 35–53. Berlin: Springer-Verlag.

Suburo AM, Scolaro JA (1990) The eye of the magellanic penguin (*Spheniscus magellanicus*): structure of the anterior segment. *Am J Anat* **189**, 245–252.

Summers AP (2000) Stiffening the stingray skeleton – an investigation of durophagy in myliobatid stingrays (Chondrichthyes, Batoidea, Myliobatidae). *J Morphol* **243**, 113–126.

Summers AP, Koob TJ, Brainerd, EL (1998) Stingrays strut their stuff. *Nature* **395**, 450–451.

Walls GL (1942) *The Vertebrate Eye and Its Adaptive Radiation*. Bloomfield Hills, MI: Cranbook Institute of Science.

Witten PE, Hall BK (2002) Differentiation and growth of kype skeletal tissues in anadromous male Atlantic salmon (*Salmo salar*). *Int J Dev Biol* **46**, 719–730.